Available online at www.sciencedirect.com
SCIENCE DIRECT®
Acta Materialia 52 (2004) 4111–4119
Acta MATERIALIA
www.actamat-journals.com

A dynamic material library for the representation of single-phase polyhedral microstructures

Veeraraghavan Sundararaghavan, Nicholas Zabaras *

Materials Process Design and Control Laboratory, Department of Mechanical and Aerospace Engineering, Sibley School of Mechanical and Aerospace Engineering, Cornell University, 188 Frank H.T. Rhodes Hall, Ithaca, NY 14853-3801, USA

Received 13 December 2003; received in revised form 10 May 2004; accepted 13 May 2004
Available online 17 June 2004

Abstract

Quantitative estimation of features from sectional images of microstructures is fundamental to determining the microstructural influences on material behavior. Geometric data extracted from planar materialographic sections through image analysis techniques are primarily lower-order descriptors of the microstructure. Such descriptors do not contain complete morphological information and hence cannot fully describe the material microstructure. This work uses a multi-class support vector machine classification method in conjunction with principal component analysis to build a dynamic and evolving microstructure library that can be used to efficiently describe single-phase polyhedral microstructures. Lower-order descriptors are initially used to associate the material microstructure to classes of microstructures stored in a digital material library. Complete description is obtained by quantifying the microstructure using the coefficients of a continuously updating basis within a class of the library. These techniques are essential towards the development of a dynamic materials library that will be able to analyze, classify and represent microstructures for modeling, accelerating the design and testing of single-phase polycrystalline materials.

Keywords: Microstructure representation; Image analysis; Principal component analysis; Dynamic microstructure library; Support vector machines

1. Introduction

Quantitative schemes for evaluating material microstructure are essential for predicting microstructure-dependent properties. Over the years, automated image analysis has been successfully used to characterize features like grain sizes and anisotropies [1] which in turn have proved useful in improving the quality of products by relating the material properties to the processing conditions. Models that attempt to predict properties rely on statistical descriptions of material microstructure [2]. Pole figures and orientation distribution functions represent crystallographic anisotropies of single-phase polyhedral microstructures [3]. Stereological parameters have been used to study the morphological anisotropy of such materials. The technique involves estimation of the three-dimensional size and shape distributions of grains through observations in planar sections using stereological equations [2,4,5]. However, in these characterization techniques, the completeness of representation has not been well studied.

Parameters such as grain size, elongation and orientation that describe single-phase polyhedral microstructures belong to the class of lower-order descriptors. Yeong and Torquato [6–8] employed lower-order descriptors such as lineal measures and two-point probability functions to reconstruct polyphase microstructures. Even though the reconstructed and reference correlation functions matched the input microstructure, the reconstructed microstructure was found to differ in other correlation measures when compared to the original microstructure. This non-uniqueness results from the absence of complete morphological information in lower-order correlation functions. It can be seen that

* Corresponding author. Tel.: +1-607-255-9104; fax: +1-607-255-9410.
E-mail address: zabaras@cornell.edu (N. Zabaras).
URL: http://www.mae.cornell.edu/zabaras/.

1359-6454/$30.00 © 2004 Acta Materialia Inc. Published by Elsevier Ltd. All rights reserved.
doi:10.1016/j.actamat.2004.05.024

parameters like the grain sizes and shapes can only provide an incomplete description of a microstructure.

This paper focuses on the completeness aspect of the description of planar images of single-phase polyhedral microstructures. Instead of looking at selective features or descriptors of the microstructure, an attempt is made to describe the microstructure as a single entity and quantitatively describe it with select set of coefficients. We employ a classification technique in conjunction with principal component analysis (PCA) for achieving a higher-order representation of microstructure images. Literature provides instances where classification is used for describing material microstructure. Tojima et al. [9] employed neural networks for the classification of graphite size in cast iron and grain sizes in stainless steel through a feature extraction method. Jenkins et al. [10] employed a decision tree-based classification scheme to describe the iron ore sinter structure. The idea behind this work was the use of a hierarchical classification structure to completely classify a microstructure based on its features. However, even though the classification scheme for a microstructure is exhaustive, the descriptors used are still lower-order terms and hence incomplete.

The automated classification structure proposed in this paper also employs lower-order descriptors like grain sizes and shape features. Nonetheless, complete description of the material microstructure is obtained by describing the microstructure through the use of a basis within a class library. In our approach, feature component vectors representing independent patterns extracted from the various classes of single-phase polyhedral microstructures are used to train a system. The classification structure evolves into a digital library through recognition of new microstructure classes and by addition of new microstructures to the existing classes. Support vector machine (SVM) is employed for effecting the automated classification of microstructures and to create the library. SVM is a successful pattern recognition technique with applications in classification, regression and time series prediction of data [11–13]. SVM outperforms classification methods like the Bayes classifier, nearest neighbor classifier and neural networks in speed and accuracy. Initial training classes consisting of ensembles of single-phase polyhedral microstructure were constructed using a Monte Carlo algorithm for grain growth. The library does not store any microstructures. Every class consists of a reduced basis which can effectively describe new microstructures. This basis evolves when new microstructures are added to the classifier and the information content of the class improves. New microstructures can be completely reconstructed through a linear combination of the basis using a set of coefficients, which are used for quantitatively representing the microstructure. A modified form of PCA extensively applied in face recognition and vision applications [14–16] has been employed for the creation of the basis. The method called incremental PCA technique [17] dynamically updates the basis within each class whenever new microstructures are added to the library.

The microstructure classification framework holds promise to the objective of automating estimation of material properties from the microstructures obtained through a real-time microstructure imaging system based on the derived set of coefficients created from the basis of the material library. Furthermore, one could potentially affiliate the microstructure classes with processes required to produce such microstructures, thus leading to an ability to select processes leading to desired microstructural features. The paper is presented in four main sections. Section 2 describes the basic image analysis methods used for feature extraction, whereas Sections 3 and 4 deal with an introduction to PCA and SVM, respectively, along with examples in relation to microstructures. In Section 5, details of implementation and results are provided.

2. Feature extraction

An automated image analysis scheme is adopted for feature extraction. For a classifier that leads to correct property calculation, it is necessary that the magnification and the rotation of the image with respect to the rolling direction are known prior to feature extraction. Raw images are initially modified so that all images in the microstructure library have the same orientation and magnification. Fig. 1 shows the important preprocessing steps such as image alignment, scaling and subsequent steps that involve sharpening the image through illumination equalization, edge enhancement and finally grain boundary detection. The boundary image can then be used in the size and shape parameter identification steps.

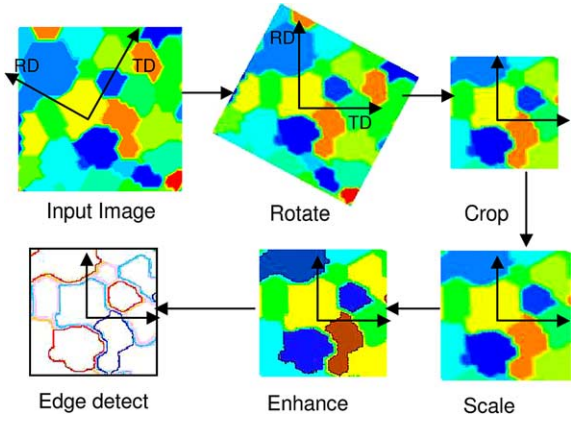

Fig. 1. Microstructure image preprocessing operations.

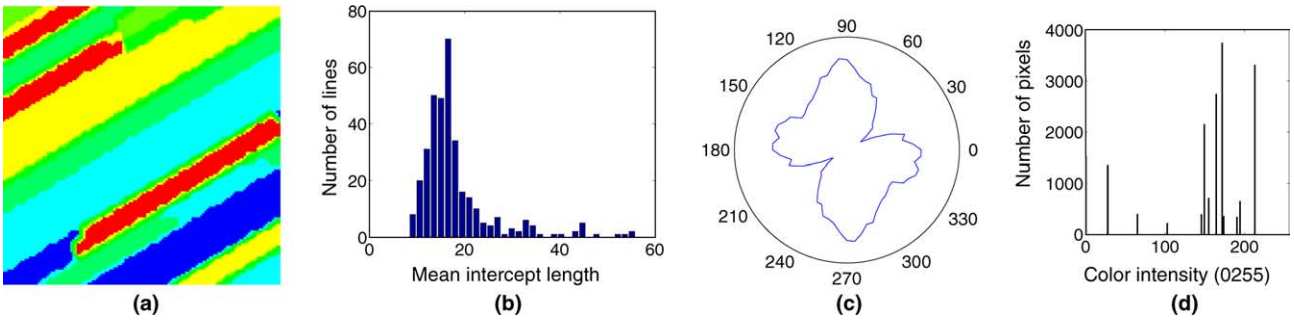

Fig. 2. (a) The input microstructure; (b) histogram of mean intercept length versus number of lines obtained using Heyn intercept technique; (c) rose of intersections and (d) color histogram of the input microstructure.

The classifier requires approximate but consistent feature vectors that can describe single-phase polyhedral microstructure features like grain sizes and shapes. The procedures for grain parameter assessment are well defined in the ASTM grain size standards, such as ASTM methods for determining average grain size (*E*, 112), for characterizing duplex grain sizes (*E*, 1181), and for determining the average grain size using semi-automated and automated image analysis (*E*, 1382).

The following three feature vectors were extracted from the input microstructure (Fig. 2(a)):

(1) Heyn's intercept technique [18,19] is employed for assessing the grain sizes. Histograms of the intercept length distribution (mean intercept length versus number of test lines possessing the mean intercept length, Fig. 2(b)) is used as the feature vector.
(2) Rose of intersections [20] (Fig. 2(c)) is used as the feature vector for assessing grain shapes.
(3) Color histogram [21] (Fig. 2(d)).

It must be mentioned that the system is not limited to the above set of descriptors. Through a hierarchical classification scheme, we include the flexibility of incorporating additional descriptors for classification. It is worth noting that the features extracted here are incapable of complete description of the microstructure since they do not contain complete morphological details of the microstructure. A method for completely representing microstructures is described in the following section.

3. Principal component analysis

Principal component analysis is a powerful method to obtain low-dimensional representation of a large amount of data. Using a set of large-dimensional data called the 'snapshots', the method decomposes the data into an optimal orthonormal basis. Few basis vectors selected in the order of importance can be used for the representation of the high-dimensional data sets. This method is well suited to the representation of microstructures and this section describes the procedure in general. Fig. 3 shows sample microstructures (I_i) used as an example for this section. The following methodology is followed to yield a low-dimensional representation of these planar microstructures. Let N different planar microstructures ($I^{(i)}$, $i = 1, \ldots, N$), each of size n pixels by n pixels are to be represented. The microstructure images are converted into N vectors ($\mathbf{X}^{(i)}$) and the average is computed as $\mu = (1/N)\sum_{i=1}^{N} \mathbf{X}^{(i)}$. The average microstructure (μ) is then subtracted from all the image vectors as $\mathbf{X}^{(i)} \leftarrow \mathbf{X}^{(i)} - \mu$, for $i = 1, \ldots, N$. The eigenvectors $\mathbf{U}^{(k)}$ of the $n^2 \times n^2$ covariance matrix $\mathbf{C} = (1/N)\sum_{i=1}^{N} \mathbf{X}^{(i)}\mathbf{X}^{(i)^{\mathrm{T}}}$ satisfying

$$\mathbf{C}\mathbf{U}^{(k)} = \lambda_k \mathbf{U}^{(k)}, \quad k = 1, \ldots, n^2, \tag{1}$$

with the eigenvalues λ_k form the best basis for the microstructures. Even though the above method calculates the best uncorrelated basis, it is computationally intensive since it involves the calculation of a correlation matrix of very large dimensionality. The work around

Fig. 3. Sample microstructures to be represented using PCA.

Fig. 4. Images of the eigenbasis: the eigen-microstructures.

this problem is the so-called 'method of snapshots'. Here, the property that the eigenvectors $\mathbf{U}^{(k)}$ are the unique linear combinations of the microstructures ($\mathbf{X}^{(i)}$) is exploited and can thus be written as

$$\mathbf{U}^{(k)} = \sum_{j=1}^{N} \alpha_{jk} \mathbf{X}^{(j)}, \quad k = 1, \ldots, N. \tag{2}$$

Let us define $\mathbf{C}^*$ as ${\mathbf{X}^{(i)}}^{\mathrm{T}} \mathbf{X}^{(j)}$, $i, j = 1, \ldots, N$, and let the vector $\mathbf{E}^{(k)} = \alpha_{ik}$, $i = 1, \ldots, N$, denote the coefficients of the eigenvector $\mathbf{U}^{(k)}$ in the basis of the snapshots. Then, the original eigenvalue problem in Eq. (1) is equivalent to the eigenvalue problem,

$$\mathbf{C}^* \mathbf{E}^{(k)} = \lambda_k^* \mathbf{E}^{(k)}. \tag{3}$$

An $N \times N$ matrix, ${\mathbf{X}^{(i)}}^{\mathrm{T}} \mathbf{X}^{(j)}$ is constructed and the vectors $\mathbf{E}^{(k)}$, $k = 1, \ldots, N$ are found from the solution of the above eigenvalue problem. The N eigenvectors $\mathbf{U}^{(k)}$ are subsequently found using Eq. (2). These vectors form the so-called 'eigen-microstructures'. The eigen-microstructures for the input microstructures in Fig. 3 are shown in Fig. 4. The eigenvectors are normalized and stored in the material library. Once the eigenbasis for the set of microstructure in the class is identified, any new microstructure corresponding to that class can be represented by transforming the microstructure into the eigenvector components by a projection operation. The coefficients (ω_k) of the new microstructure (Γ) in the normalized eigenbasis are given by

$$\omega_k = {\mathbf{U}^{(k)}}^{\mathrm{T}} (\Gamma - \mu), \quad k = 1, \ldots, N. \tag{4}$$

The coefficients (ω_k) form a vector $\Omega = [\omega_1, \ldots, \omega_N]^{\mathrm{T}}$ that is used as a reduced representation for the microstructure. The matrix of coefficients of the input microstructures $[\Omega_1, \ldots, \Omega_N]$ is denoted by $\mathbf{A}$, the representation matrix. The representation matrix for the input microstructures of Fig. 3 in the eigenbasis of Fig. 4 is listed in Table 1.

Table 1
Coefficients ($\mathbf{A}$) of the input microstructures in the eigenbasis ($\times 0.001$)

0.0125	1.3142	−4.23	4.5429	−1.6396
−0.8406	0.8463	−3.0232	0.3424	2.6752
3.943	−4.2162	−0.6817	−0.9718	1.9268
1.1796	−1.3354	−2.8401	6.2064	−3.2106
5.8294	5.2287	−3.7972	−3.6095	−3.6515

4. Support vector machines

Microstructures with similar features can be represented by a set of coefficients in a reduced basis using PCA. The aim of classification is to group similar microstructures within a class where PCA may be carried out efficiently (i.e., with a reduced number of eigen-microstructures). For clarity of the presentation, the discussion here is limited to binary classification. The classification problem has been solved using SVM. SVM is a statistical learning algorithm for pattern classification and regression [22]. The classification involves prior training with features from known microstructure classes. The training involves finding the optimal hyperplane such that the error for unseen test microstructures is minimized. Each instance in the training set consists of class labels and several attributes extracted from the microstructure. The goal of SVM is to produce a model which predicts the class of the data set given in the form of features. Given a training set of feature-class pairs $(\mathbf{x}_i, y_i)$, $i = 1, \ldots, \ell$, where $\mathbf{x}_i \in \Re^m$ and $y_i \in \{1, -1\}$, the SVMs non-linearly maps the data $\mathbf{x}$ to a higher-dimensional feature space F as $\mathbf{z} = \phi(\mathbf{x})$. The function $\phi(\mathbf{x})$ is defined by a positive definite kernel, $K(\mathbf{x}_1, \mathbf{x}_2)$, specifying an inner product in the feature space, $\phi(\mathbf{x}_1) \cdot \phi(\mathbf{x}_2) = K(\mathbf{x}_1, \mathbf{x}_2)$. The kernel employed for microstructure classification is the linear kernel, $K(\mathbf{x}_1, \mathbf{x}_2) = \mathbf{x}_1 \cdot \mathbf{x}_2$. If the data are linearly separable in F, a decision function $D(\mathbf{x}) = \mathbf{w} \cdot \phi(\mathbf{x}) + b$, where $\mathbf{w}$ is an m-dimensional vector and b is a scalar, can be determined such that,

$$y_i D(\mathbf{x}_i) \geqslant 1, \quad i = 1, \ldots, \ell. \tag{5}$$

The distance from the separating hyperplane $D(\mathbf{x}) = 0$ and the training datum nearest to the hyperplane is called the margin. The hyperplane with the highest margin is called the optimal hyperplane. Fig. 5 shows a realization of a binary classifier through the creation of a hyperplane that maximizes the margin between the two examples. The vector $\mathbf{w}$ for the optimal hyperplane is obtained by maximizing the margin which becomes equivalent to minimizing $\|\mathbf{w}\|$. The solution to this is given by

$$\mathbf{w} = \sum_{i=1}^{\ell} \alpha_i y_i \phi(\mathbf{x}_i) \quad \text{for } \alpha_i \geqslant 0.$$

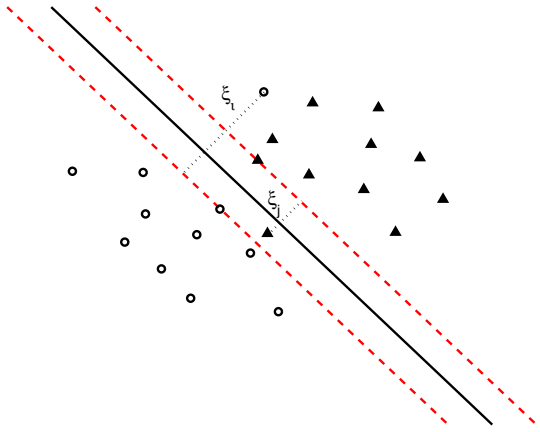

Fig. 5. Support vectors (shown as dotted lines) used for binary classification in a non-separable case. The slack variables (ξ) are used to minimize the training error while maximizing the margin.

The problem of determining the α_i's is posed as a quadratic programming problem of maximizing,

$$W(\alpha) = \sum_{i=1}^{\ell} \alpha_i - \frac{1}{2} \sum_{i,j=1}^{\ell} y_i y_j \alpha_i \alpha_j K(\mathbf{x}_i, \mathbf{x}_j), \tag{6}$$

in the positive quadrant $\alpha_i \geqslant 0$, $i = 1, \ldots, \ell$, subject to the constraint, $\sum_{i=1}^{\ell} \alpha_i y_i = 0$. The optimal b is then found as $b = y_i - \mathbf{w} \cdot \mathbf{x}_i$, where $i = \arg\max_k(\alpha_k)$. The support vectors are the points for which $\alpha_i > 0$ satisfying Eq. (5) with equality. Given a new microstructural feature $\mathbf{x}$, the decision function which gives the class $y_i \in \{1, -1\}$ can be written as

$$f(\mathbf{x}) = \operatorname{sgn}\left(\sum_{i=1}^{\ell} \alpha_i y_i K(\mathbf{x}_i, \mathbf{x}) + b \right). \tag{7}$$

When the data are non-separable in the higher-dimensional feature space, slack variables $\xi_i \geqslant 0$ are introduced such that $y_i D(\mathbf{x}_i) \geqslant 1 - \xi_i$, $i = 1, \ldots, \ell$ to allow the possibility of samples to violate Eq. (5). Fig. 5 shows the optimal hyperplane with the slack variables (ξ_i) indicated. The idea is to simultaneously maximize the margin and minimize the training error (represented by the slack variables). The generalized optimal separating hyperplane is then the minimization of $(1/2)\|\mathbf{w}\|^2 + C\sum_{i=1}^{\ell} \xi_i$, where the purpose of C in the second term is to control the number of misclassified points.

4.1. Multi-class support vector machines

Microstructure classification is a multi-class problem with classification based on multiple feature parameters like grain sizes and shapes. The one-against-one method has been employed for this classification problem [23]. If between two classes i and j, a given data set is classified to class i, then the vote for class i is incremented by one. Given k classes of microstructures, this method constructs $k(k-1)/2$ classifiers, where each classifier is trained on data from two classes. A new data point is classified to the class which obtains the maximum votes. In case that two classes have identical votes the class with a smaller index is selected. A study [24] indicates that this method is more effective than other multi-class SVM techniques like 'one-against-all' and 'all-together' methodologies. Given a new microstructure that does not belong to the existing classes, the SVM classifier places the microstructure into the class k in which the feature sets are closest to the input feature vector ($\mathbf{x}$). An ad hoc method that allows creation of new classes from such microstructures is the calculation of a distance measure (ϵ_k) between the input feature vector ($\mathbf{x}$) and the average feature vector ($\mathbf{x}_k$) of the class k as, $\epsilon_k = \|\mathbf{x} - \mathbf{x}_k\|_2$. If the distance ϵ_k is above a chosen threshold, the feature is optionally used to create a new class and the classifier is retrained to create new support vectors of the class. Fig. 6 shows the distance of the roses of intersection feature vector of four representative class microstructures from the average feature vector of a class. The feature vector of microstructure (a) exceeds the threshold ($\epsilon_k > 30$) and is used to create a new class. This is followed by retraining of the classifier. The retraining process realigns the support vectors so that the new class can be separated from the other classes. An iterative online training procedure where the alignment of the support vectors are gradually improved with

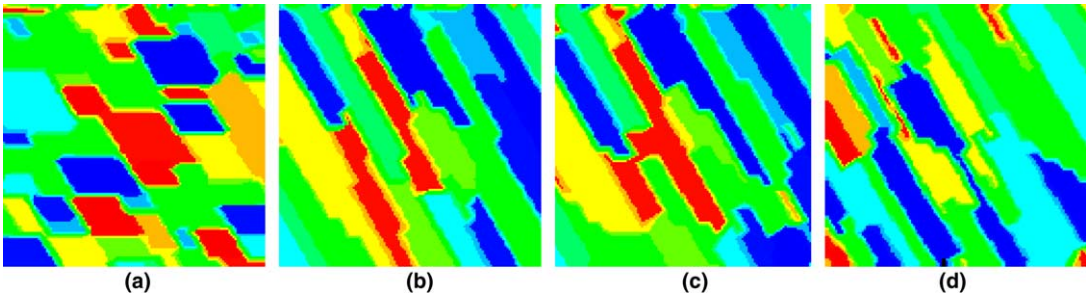

Fig. 6. (a–d) Microstructures classified to the same class. The distance of the average feature vector of the class from the input microstructure feature vector is indicated below each microstructure. A new class is created to accommodate microstructure (a).

addition of training data is another option but is not addressed in this work.

5. Implementation and results

The microstructures used in this study have been generated using a Monte Carlo grain growth model. Mehnert et al. [25] employed a similar Monte Carlo simulator for generating samples of microstructure for the stereological problem of estimating the spatial grain size distribution from planar microstructures. The model provides a representative set of polyhedral microstructures similar to the complex microstructures encountered in reality. Using the features of these microstructures as the training data sets, SVMs identify the representative classes of new and unknown microstructures. Fig. 7 describes the two class hierarchical structure of the library. Microstructures are first classified according to the shape of grains in the top tier of the library. Classes of microstructures having similar grain shapes are further divided into sub-classes based on the constituent grain sizes. The hierarchical class structure can be expanded by further dividing the grain size classes based on additional microstructure-specific features.

Even though Fig. 7 depicts microstructure images associated with the classes, in practice none of the images are stored in the library. The lowest class level (the grain size classes corresponding to each shape class in Fig. 7) holds an eigenbasis which contains information about the microstructures (see Section 5.2).

5.1. Testing of the classifier's accuracy

To test the classification scheme employed, 375 images of microstructures were created using the Monte Carlo grain growth model. Each microstructure image was sized to 128×128 pixels with 256 intensity levels. For testing the accuracy of classification, we do not allow creation of new classes. The classifier is tested within a fixed set of 11 classes of microstructures created based on grain shapes. The roses of intersection of the microstructures were normalized in the range $[-1, 1]$ and were used as feature vectors. Randomly selected images were employed for training the classifier. It is ensured that the training and the test sets do not overlap. The classifier was repeatedly trained using random sets of 40 microstructures and the classifier accuracy was checked using the rest 335 microstructures as test examples. On an average, the multi-class SVM classification scheme gave an accuracy of 92.53%, with the lowest accuracy of 87.76% and highest accuracy of 95.82% for 30 training runs. When the number of training examples was increased to 100, the classifier was able to achieve an average accuracy of 95.80%.

5.2. Representation over the eigenbasis

Once the initial class structure for the library is created, an eigenbasis is created at the last level in the class hierarchy. The possibilities that arise when a new microstructure is given to the library for representation are:

(1) The new microstructure is classified to an already existing class in the library.
   (a) No new information is gained from the microstructure. The existing basis is used for representing the microstructure.
   (b) Microstructure contains additional information about the class. The basis is updated to accommodate the new information (see Section 5.3). In addition, the representation coefficients in the new basis of the images used to generate

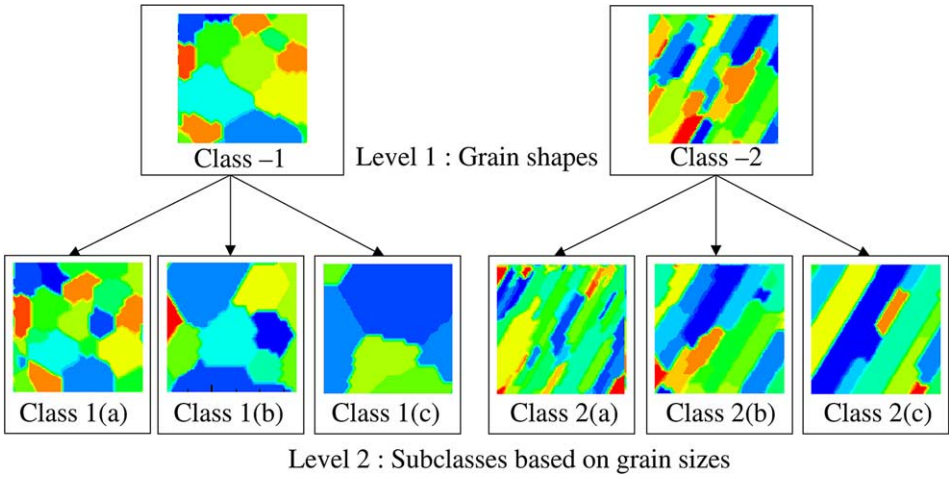

Fig. 7. An example of hierarchical classification structure: In level 1, microstructures are classified according to grain shapes. In level 2, microstructures in each shape class are subdivided into three more classes according to the grain sizes.

the old basis and of the new microstructure are computed and stored.

(2) The microstructure does not belong to any of the existing classes. A new class is created along with an initial basis for the class.

When a new class is created, the first microstructure in the class is used to create an initial eigenbasis for the class by assigning the mean $\mu = X_1$, the initial eigenbasis $U = [0, \ldots, 0]_{128^2 \times 1}$ and the representation coefficient $\mathbf{A} = 0$, where X_1 is the image vector of size $128^2 \times 1$. The basis is then continuously updated based on new microstructures that contain additional information about the class of microstructures.

The coefficients over a fraction of the eigenbasis is normally sufficient for complete representation of a microstructure. Fig. 8 shows a microstructure reconstructed within a class using different fractions of eigenvectors in the basis. It can be seen that a reconstruction of good quality is possible even when 40% of the eigenvectors are not used for the reconstruction.

Fig. 9 shows the eigenvalues based on PCA of a class of 25 microstructures. Eigenvalues decay rapidly and most of the 'energies' are concentrated in the first few eigenvalues. The eigenvectors corresponding to the smaller eigenvalues can be discarded to achieve a more compact representation.

5.3. Dynamic update of eigenspaces

Whenever a new microstructure (Γ_k) of size (128×128) is added to a class of microstructures, the existing basis (U) is first used to reconstruct the microstructure. We use a distance measure (d) to test if the microstructure contains any new information that can be used to improve the information contained in the class basis. This measure is based on the Frobenius norm of the difference between the test microstructure (Γ_k) and the reconstructed microstructure (Γ_k^{R}) and is given by

$$d = \frac{\|\Gamma_k - \Gamma_k^{\mathrm{R}}\|_F}{128}. \tag{8}$$

The gray level intensities of the test microstructure and the reconstructed microstructure were normalized within limits of $[0, 1]$. If d is less than 0.1, the microstructure is assumed to add no new information to the existing basis and after it is represented in the old basis is discarded. If $d > 0.1$, the basis is updated to accommodate the new information contained in the microstructure. The microstructure is represented based on the updated basis.

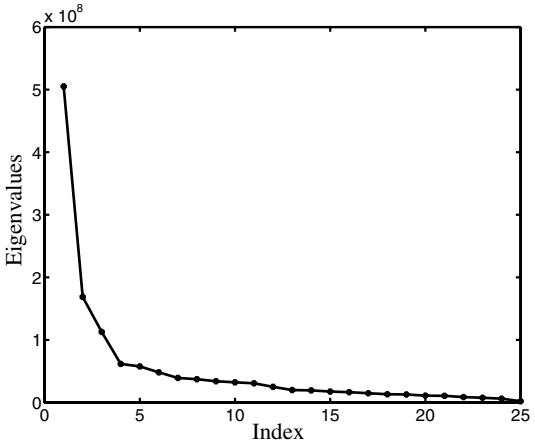

Fig. 9. Eigenvalues of the correlation matrix.

In the dynamic library, we foresee representation of microstructures sequentially in real-time. The PCA technique described in Section 3 is performed in the batch mode. Generation of the updated eigenbasis using batch PCA would be computationally prohibitive since the analysis is based on a set of high-dimensional image data.

To avoid operations on higher-dimensional images, we employ an incremental PCA technique proposed by Skočaj and Leonardis [17] for the dynamic update of the eigenbasis. As discussed earlier, the microstructures are discarded after a PCA update and only the coefficients of the microstructures are stored along with the updated eigenbasis. The implemented technique summarized in Table 2 provides the framework for online representation of microstructures. The PCA performed on the coefficient matrix $\mathbf{A}'$ is similar to the PCA in Section 3 but using the columns of the coefficient matrix instead of the images $\mathbf{X}^{(i)}$.

The representation format of a microstructure in the dynamic material library is shown in Table 3. The representation includes information about the lower-order

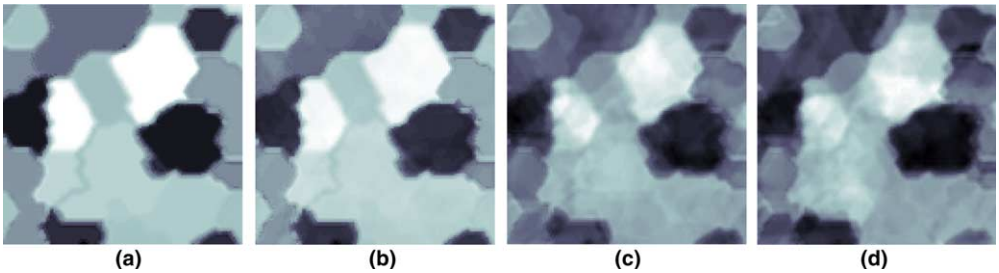

Fig. 8. Microstructure reconstructed using PCA with: (a) 100% of the basis; (b) 80% of the basis; (c) 60% of the basis and (d) 40% of the basis.

Table 2
Principal component analysis: algorithm for incremental basis update [17]

Inputs at update step $(n+1)$: current mean of existent images in the class $\mu^{(n)}$, current eigenvectors $\mathbf{U}^{(n)}$, current coefficients of existent class images $\mathbf{A}^{(n)}$, new input image $\mathbf{X}$
Outputs: updated mean $\mu^{(n+1)}$, eigenvectors $\mathbf{U}^{(n+1)}$ and coefficients $\mathbf{A}^{(n+1)}$
Project the new image $\mathbf{X}$ in the current eigenbasis: $\mathbf{a} = \mathbf{U}^{(n)\mathrm{T}}(\mathbf{X} - \mu^{(n)})$.
Reconstruct the new image: $\mathbf{Y} = \mathbf{U}^{(n)}\mathbf{a} + \mu^{(n)}$
Compute the residual vector: $\mathbf{r} = \mathbf{X} - \mathbf{Y}$
Append $\mathbf{r}$ as the new basis vector: $\mathbf{U}' = \left[\mathbf{U}^{(n)}, \frac{\mathbf{r}}{\|\mathbf{r}\|}\right]$
Form $\mathbf{A}'$ as follows: $\mathbf{A}' = \begin{pmatrix} \mathbf{A}^{(n)}, & \mathbf{a} \\ 0, & \|\mathbf{r}\| \end{pmatrix}$
Perform PCA on $\mathbf{A}'$ and obtain the mean μ'' and the eigenvectors $\mathbf{U}''$.
Update the coefficients: $\mathbf{A}^{(n+1)} = \mathbf{U}''^{\mathrm{T}}(\mathbf{A}' - \mu''\mathbf{1}_{1\times(n+1)})$
Update the basis: $\mathbf{U}^{(n+1)} = \mathbf{U}'\mathbf{U}''$
Update the mean: $\mu^{(n+1)} = \mu^{(n)} + \mathbf{U}'\mu''$

Table 3
Representation format for a microstructure in the library

Date: 12/7 2:45PM, Basis updated
Shape class: 4 (Description: oriented 45°, elongated)
Size class: c (Description: large grains)
Basis coefficients: (Size class c of shape class 4): [12.06, 4.32, −5.45, 16.54, 2.75]

descriptors like grain shapes and sizes, along with additional data in the form of PCA representation coefficients for complete description of the microstructure. Fig. 10 illustrates the importance of classification in the context of microstructure representation. Fig. 10(a) shows a new microstructure assigned to a class by the SVM classifier. Fig. 10(b) shows the reconstruction achieved using six coefficients (24% of the updated basis) in the class containing 25 eigenvectors. After the number of eigenvectors in the class had expanded to accommodate information content of 60 images, the microstructure was once again given as a test example for reconstruction. Fig. 10(c) shows the new reconstructed image, once again using six coefficients (10% of the basis). The improvement in the representation can be attributed to an enhancement in the information content of the basis whenever microstructures with similar lower-order (shape) attributes are used to update the class basis. As it is expected, with the number of microstructures used to generate the eigenbasis increasing, the quality of representation of other images increases when using a fixed number of eigenvectors.

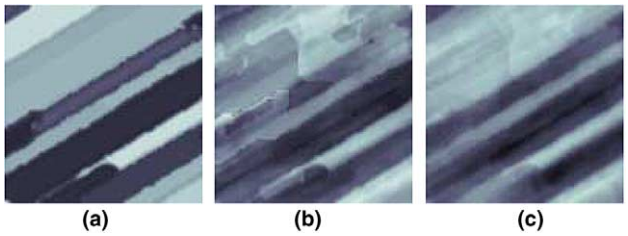

Fig. 10. (a) New microstructure; (b) microstructure reconstructed using six coefficients in a class of 25 eigenvectors and (c) reconstruction using six coefficients over the expanded class of 60 eigenvectors.

Misclassification and insufficient classification can deteriorate the basis. Improved feature selection and classification schemes need to be developed to address such problems. Efficient PCA representation can also be obtained through several levels of class refinement to limit large variations in microstructures within a class.

6. Conclusions

The problem of completeness of microstructure representation is addressed in this paper by demonstrating a classification based representation scheme for single-phase polyhedral microstructures based on a dynamic microstructure library. SVMs are used to classify microstructures based on the grain size and shape features. The classification structure evolves into a library of microstructures through recognition of new classes and by addition of information to the existing classes through new microstructures. The lowest level in the class hierarchy holds a eigenbasis for representing microstructures. The basis dynamically updates with the arrival of new microstructures within a class and the information content of the basis improves. Complete microstructure representation is achieved through a set of coefficients in the generated basis. Through continuous training, the dynamic microstructure library is capable of recognizing and completely representing any single-phase polyhedral microstructure.

Acknowledgements

The authors acknowledge Dr. J. Simmons, AFRL/MLLMP for providing the background material needed to initiate this work. The work presented here was funded by AFOSR (Grants F49620-00-1-0373 and FA9550-04-1-0070) and by the NSF (Grant DMI-0113295). This research was conducted using the resources of the Cornell Theory Center.

References

[1] Wojnar L. Image analysis – applications in materials engineering. Boca Raton: CRC Press; 1999.
[2] Ohser J, Mücklich F. Statistical analysis of microstructures in materials science. New York: Wiley; 2000.

[3] Kocks UF, Tóme CN, Wenk HR. Texture and anisotropy: preferred orientations in polycrystals and their effect on materials properties. Cambridge: Cambridge University Press; 1998.
[4] Underwood EE. Quantitative stereology. Reading: Addison-Wesley; 1970.
[5] Hilliard JE, Lawson LR. Stereology and stochastic geometry. Dordrecht: Kluwer Academic Publishers; 2003.
[6] Yeong CLY, Torquato S. Phys Rev E 1998;57(1):495.
[7] Yeong CLY, Torquato S. Phys Rev E 1998;58(1):224.
[8] Torquato S. Ann Rev Mater Res 2002;32:77.
[9] Tojima M, Suzuki T, Kobayashi F. Classification of graphite shapes in cast irons using neural networks. In: COMP '93, international conference on computer-assisted materials design and process simulation proceedings, Tokyo (Japan). Japan: Iron and Steel Institute; 1993. p. 463.
[10] Jenkins BM, Lovel RR, Thurlby JA. Quantification of iron ore sinter structure by optical image analysis. In: Vander Voort GF, editor. MiCon 90: advances in video technology for microstructural control ASTM STP 1094. Philadelphia: American Society for Testing and Materials; 1990. p. 292.
[11] Lia S, Kwoka JT, Zhu H, Wang Y. Pattern Recogn 2003;36:2883.
[12] Pontil M, Verri A. IEEE Trans Pattern Anal Mach Intell 1998;20(6):637.
[13] Dumais S. IEEE Intell Systems 1998;13(4):21.
[14] Turk M, Pentland A. J Cognitive Neurosci 1991;3(1):71.
[15] Samal A, Iyengar PA. Int J Pattern Recog Artif Intell 1995;9(6):845.
[16] Sirovich L, Kirby M. J Opt Soc Am 1987;4:519.
[17] Skočaj D, Leonardis A. Incremental approach to robust learning of eigenspaces. In: Leberl F, Fraundorfer F, editors. 26th workshop of the Austrian Association for Pattern Recognition (AGM/AAPR). Graz (Austria): Sterreichische Computer Gesellschaft; 2002. p. 71.
[18] Vander Voort GF. Examination of some grain size measurement problems. In: Vander Voort GF, Warmuth FJ, Purdy SM, Szirmae, editors. Metallography: past, present and future (75th anniversary volume) ASTM STP 1165. Philadelphia: American Society for Testing and Materials; 1993. p. 266.
[19] Vander Voort GF. Metallography: principles and practice. New York: McGraw-Hill; 1984.
[20] Saltykov SA. Stereometrische metallographie. Leipzig: Deutscher Verlag fur Grundstoffindustrie; 1974.
[21] Chapelle O, Haffner P, Vapnik V. IEEE Trans Neural Network 1999;10(5):1055.
[22] Vapnik VN. Statistical learning theory. New York: Wiley; 1998.
[23] Chang CC, Lin CJ. LIBSVM: a library for support vector machines 2001. Available from: http://www.csie.ntu.edu.tw/~cjlin/libsvm.
[24] Hsu CW, Lin CJ. IEEE Trans Neural Network 2000;13:679.
[25] Mehnert K, Ohser J, Klimanek P. Mater Sci Eng 1998;A246:207.